

Distilling Token-Trained Models into Byte-Level Models

Zishuo Bao^{1*} Jiaqi Leng² Junxiong Wang³ Bowen Peng⁴ Yucheng Lu⁵

Abstract

Byte Language Models (BLMs) have emerged as a promising direction for scaling language models beyond tokenization. However, existing BLMs typically require training from scratch on trillions of bytes, making them prohibitively expensive. In this paper, we propose an efficient distillation recipe that converts existing token-trained LLMs into BLMs while retaining comparable capabilities. Our recipe follows a two-stage curriculum: (1) *Progressive Knowledge Distillation*, which aligns byte-level representations with the embeddings of the token-trained teacher model; and (2) *Byte-Level Supervised Fine-Tuning*, which enables end-to-end generation entirely in the byte space. We validate our approach across multiple model families, including Llama, Qwen, and OLMo, and demonstrate that the distilled BLMs retain most of the teacher models' performance using only approximately 125B bytes.

1. Introduction

Recent developments have witnessed a surge of interest in Byte Language Models (BLMs), which operate directly in the byte space by consuming and generating bytes, thereby eliminating the inductive bias imposed by tokenization. A growing body of work has demonstrated that modeling language at the byte level can achieve strong performance while mitigating tokenization-induced artifacts (Nawrot et al., 2022; 2023b; Yu et al., 2023; Slagle, 2024; Ho et al., 2024; Wang et al., 2024a; Pagnoni et al., 2024; Hwang et al., 2025).

A common thread across these successful architectures is the use of a *hierarchical structure*: they typically leverage a lightweight encoder to first compress raw bytes into chunks, which are then processed by a transformer backbone before being decoded back into bytes. This structural similarity to standard Large Language Models (LLMs) suggests a

natural opportunity for knowledge transfer. In particular, it enables initializing the transformer backbone from powerful pretrained token-based (subword) LMs.

However, while several prior works explore initializing byte-level models with weights from pretrained token-trained LMs to accelerate convergence (Hwang et al., 2025; Pagnoni et al., 2024), these approaches have not succeeded in closing the performance gap: the resulting BLMs still substantially underperform their token-based counterparts. To address this gap, in this paper we study the following question:

Can we obtain a byte-level model through distillation from a token-trained model, without training from scratch?

We answer this question in the affirmative by proposing a novel distillation recipe. Our approach distills a standard Transformer-based language model into a hierarchical byte-level model, such as H-Net (Hwang et al., 2025). The central challenge here lies in the boundary mismatch between the two representations: token-based models impose fixed, discrete boundaries over raw byte sequences, whereas byte models dynamically group bytes into variable-length units. This mismatch falls outside the scope of traditional distillation methods, which typically assume a fixed and shared output space. To resolve this, as illustrated in Figure 1, we introduce a two-stage distillation pipeline that progressively aligns fine-grained byte-level representations with pretrained token embeddings. Unlike prior approaches that rely on extensive retraining from scratch, our method follows a structured curriculum:

Stage 1: Progressive Knowledge Distillation. The main challenge in distillation arises from mismatched boundaries between LLMs and BLMs in byte space. We address this challenge with a three-stage process: (1) embedding alignment, (2) joint distillation, and (3) boundary learning, which trains the student model to process raw bytes while faithfully mimicking the teacher model's token-level outputs. This stage allows the distilled BLM to take raw bytes as inputs and generate in the token space.

Stage 2: Byte-Level Supervised Fine-Tuning (SFT). Building on Stage 1, we introduce a dechunking module and apply supervised fine-tuning (SFT) with a next-byte prediction objective, enabling the model to generate entirely in the byte space.

*Work done during the internship at NYU Shanghai.
¹Fuzhou University ²Fudan University ³Together AI ⁴Nous Research ⁵NYU Shanghai. Correspondence to: Yucheng Lu <lu.yucheng@nyu.edu>.

We substantiate our recipe over a variety of model families, including Llama (Grattafiori et al., 2024), Qwen (Yang et al., 2025) and OLMo (OLMo et al., 2024). The empirical results demonstrate unprecedented data efficiency. With approximately 125 B training bytes in total, our distilled model retains the vast majority of teacher models’ capabilities in downstream tasks. For instance, on the MMLU benchmark, our method achieves scores of 51.8 and 68.5 for Llama-3.2 3B and Qwen-3 4B respectively, retaining over 92% of the original performance. This represents a significant reduction in resource consumption compared with state-of-the-art baselines.

Our main contributions in this paper can be summarized as follows:

- We propose a novel two-stage distillation framework that effectively transforms token-trained LLMs into BLMs, which drastically reduces the data requirement compared with training BLMs from scratch.
- We validate our approach across various models (including Llama, Qwen, and OLMo). Furthermore, we explore post-training strategies, demonstrating that *On-Policy Distillation* can further enhance the student model’s capabilities.
- We validate the effectiveness of our architectural choices through extensive ablation. Furthermore, we provide a comprehensive analysis of the intrinsic characteristics and behaviors of the distilled student models on byte-level tasks.
- We open-source all components of our recipe, including the distillation code and pretrained model checkpoints, for the community to build upon¹.

2. Related Work

2.1. Efficient Byte-Level Architectures

Directly modeling raw bytes removes the biases associated with tokenization but presents significant computational challenges due to the quadratic complexity of self-attention over extended sequences. To mitigate this, recent research has explored various architectural innovations that can generally be divided into *isotropic* and *hierarchical* approaches.

Isotropic architectures process the full byte sequence without downsampling, typically employing linear-time mechanisms to bypass the cost of standard attention. For instance, Wang et al. (2024a) leverages Selective State Space Models (SSMs) for linear efficiency. In contrast, *hierarchical architectures* aim to reduce the effective sequence length by grouping bytes into coarser chunks, thereby enabling the use of standard transformer backbones. The most straightforward realization of this is *static chunking*, where models

such as Nawrot et al. (2022), Yu et al. (2023), Ho et al. (2024), Yu et al. (2023), and Egli et al. (2025) partition inputs into fixed-size chunks. Although computationally efficient, these content-agnostic boundaries often disrupt meaningful semantic units. To preserve semantic integrity, *external chunking* strategies define boundaries using heuristics or auxiliary signals. Slagle (2024) segments text based on natural delimiters such as whitespace, whereas Nawrot et al. (2023a) and Pagnoni et al. (2024) employ an entropy-based mechanism to identify information-dense transitions. Finally, *dynamic chunking* offers the most flexible solution by learning the segmentation boundaries end-to-end within the model itself. Hwang et al. (2025) exemplifies this approach by utilizing a learnable routing module to segment sequences based on intrinsic semantic granularity. We adopt H-Net as our backbone to leverage this balance between efficiency and linguistic plausibility.

2.2. Token-to-Byte Knowledge Distillation

Hinton et al. (2015) is a fundamental technique for transferring capabilities from a teacher model to a student model. Prior work has explored cross architecture distillation (Kasai et al., 2021; Wang et al., 2024b) from Transformers (Vaswani et al., 2017) to linear RNNs (Katharopoulos et al., 2020; Dao & Gu, 2024) or hybrid models. However, while KD can transfer knowledge across architectures when the tokenizer is same, distilling knowledge from token to byte poses unique challenges due to boundary misalignment introduced by varying vocabularies and sequence lengths (Minixhofer et al., 2025b).

In the realm of byte-level modeling, early strategies such as Pagnoni et al. (2024) leverage weights from pretrained token models (e.g., Llama-2 7B) to initialize their latent transformers. Similarly, Hwang et al. (2025) begins with weights of token LMs and incorporates auxiliary losses for alignment. However, these methods are essentially SFT. As a result, they still demand significant data to replicate teacher models’ capabilities.

Concurrent to this paper, Bolmo introduced a “byteification” process that employs a direct distillation strategy (Minixhofer et al., 2025a), which makes the first attempt with multiple approximation methods for vocabulary and sequence alignment. Although these approximations work well for OLMo families (OLMo et al., 2024; Olmo et al., 2025), their applicability to other model families remains uncertain, likely necessitating substantial manual hyperparameter tuning across different settings.

3. Preliminary

We develop our distillation recipe on a representative hierarchical byte model named H-Net (Hwang et al., 2025).

¹<https://github.com/heavyball-research/DistillBytes>

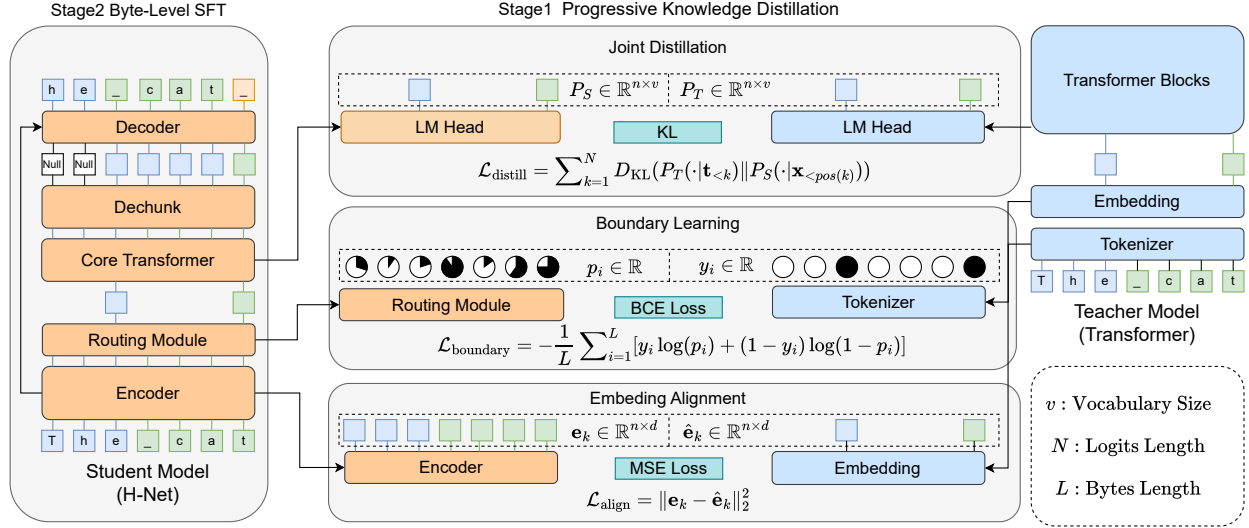


Figure 1. Overview of the Two-Stage Distillation Framework. **Stage 1: Progressive Knowledge Distillation** includes: (a) *Embedding Alignment* to map byte patches to the token space (L_{align}); (b) *Joint Distillation* to synchronize hidden states and logits ($L_{distill}$); (c) *Boundary Learning* to align tokenization via the One-Byte Lookahead Router ($L_{boundary}$). **Stage 2: Full Byte-Level SFT** enables end-to-end generation in the byte space via Dechunk and Decoder modules.

Such recipe can be easily extended to other hierarchical byte models. Here we provide a short overview for H-Net architecture.

H-Net is a U-Net-like architecture crafted for multi-granularity sequence modeling. As illustrated in left hand side of Figure 1, it employs a hierarchical data flow: raw byte sequences are first processed by an encoder, compressed into a much shorter sequence of latent chunks (e.g. group of bytes), and then expanded back to the original byte-level resolution using a decoder.

The core of this architecture is the *Dynamic Chunking* mechanism. A routing module predicts the adaptive boundary probabilities for each position, segmenting the sequence into compressed representations that encapsulate higher-level semantic information. During reconstruction, a smoothing module interpolates these representations to restore the original resolution while maintaining end-to-end differentiability. To preserve fine-grained details, H-Net integrates a residual connection that projects the initial encoder outputs directly to the dechunking stage, effectively bridging the gap between the local byte-level features and the global context.

4. Methodology

In this section, we introduce our main distillation recipe. We start by illustrating the adaptions made to the original H-Net architecture (student model), which ensures alignment that is essential for distillation (4.1). Subsequently, we propose a two-stage framework to systematically align byte-level

representations with the teacher model’s semantic space and allow the model to generate end-to-end in the byte space (4.2).

4.1. Student Model Architecture Design

4.1.1. ONE-BYTE LOOKAHEAD ROUTING

In standard dynamic chunking, the start of a chunk is typically identified as the boundary. However, to align with the tokenization behavior, it is more intuitive to define the boundary at the end of each chunk. To achieve this, we introduce a *one-byte lookahead* mechanism in the Routing Module.

Instead of predicting the boundary probability p based solely on the current state, our router computes the similarity between the *current* byte hidden state \mathbf{x}_{curr} and the *next* byte hidden state \mathbf{x}_{next} as follows:

$$p = 1 - \frac{1}{2} \cdot \frac{\mathbf{x}_{curr}^\top \mathbf{x}_{next}}{\|\mathbf{x}_{curr}\| \|\mathbf{x}_{next}\|} \quad (1)$$

On top of which a boundary indicator $b = \mathbb{I}(p \geq 0.5)$ is derived, which marks the end of a chunk. This lookahead mechanism ensures that the hidden state for each byte aggregates information up to the closure of the current chunk before entering the core transformer.

4.1.2. DECODING STRATEGY

Although the one-byte lookahead routing described above is effective during the parallel prefill stage, it hinders autoregressive generation as future bytes are unavailable. To

reconcile the need for lookahead with the causality constraints of inference, we explore two distinct strategies to predict boundaries in decoding.

Joint Boundary Prediction (JBP). A straightforward approach, introduced in Bolmo (Minixhofer et al., 2025a), encodes boundary information directly into the output vocabulary. Specifically, the decoder’s vocabulary is expanded to $\mathcal{V}_{\text{total}} = \mathcal{V}_{\text{byte}} \times 2$, where each byte is paired with a boundary indicator. At each generation step t , the model predicts a logit $y_t \in 0, \dots, 511$ that jointly represents the next byte and its boundary status: values in $[0, 256]$ indicate an internal byte, while values in $[256, 512)$ mark a chunk boundary. The model is trained end-to-end to generate directly in this augmented space.

Multi-Byte Prediction (MBP). Alternatively, we propose a Multi-Byte Prediction mechanism designed to explicitly simulate the lookahead behavior of the router during inference. Because our routing logic relies on comparing the current byte with the *next* byte to determine a boundary, we introduce an auxiliary language modeling head alongside the primary head.

At time step t , whereas the primary head predicts the next byte x_{t+1} , the auxiliary MBP head is trained to predict the *next-next* byte x_{t+2} . This auxiliary prediction serves a specialized purpose: it provides a proxy for the future state required by the routing module. By feeding the predicted embedding of x_{t+2} into the router, the model can compute the boundary probability for x_{t+1} using the same look-ahead logic, effectively maintaining consistency between training and inference without violating causality.

4.1.3. ENSURING GENERATION CAUSALITY WITH SHIFTED UP-SAMPLING

To map chunk-level representations back to the byte space, we employ a Dechunk module that upsamples chunk representations $H = [h_1, \dots, h_N]$ into byte-level states $U = [u_1, \dots, u_L]$. Because each chunk representation h_k aggregates information from its entire chunk, naively broadcasting it to all corresponding byte positions would leak future information (Pagnoni et al., 2024).

Following the dynamic pooling strategy of (Nawrot et al., 2023b), we avoid this issue by revealing h_k only at the final byte of the k -th chunk. For non-final bytes, the model instead uses the representation of the previous chunk (or a learned NULL state for the first chunk). This preserves the autoregressive property while providing maximal context at chunk boundaries.

4.2. Two-stage Distillation Framework

With the modification to H-Net, we propose a unified framework for transferring knowledge from a token-trained

teacher model to a byte-level student model. As illustrated in our pipeline in Figure 1, this framework is structured into two distinct phases: *Stage 1*, which focuses on progressive representation alignment and boundary learning; and *Stage 2*, which transitions the model to generate entirely in the byte space.

4.2.1. STAGE 1: PROGRESSIVE KNOWLEDGE DISTILLATION

The main challenges in the distillation process are the *vocabulary* and *sequence length* mismatch: while the teacher model operates on discrete semantic tokens, the student model must learn to derive these chunks from raw byte sequences. To address this, we design three specific loss objectives to align the student model’s embedding space, semantic probabilities, and boundary decisions with those of the teacher model, which are illustrated in the middle of Figure 1.

Loss Definitions. First, to handle mismatches, we define the *Embedding Alignment Objective* ($\mathcal{L}_{\text{align}}$). For a byte span corresponding to a token t_k , we minimize the difference between the hidden state of the student model encoder at the boundary byte $\hat{\mathbf{e}}_k$ and the static embedding of the teacher model \mathbf{e}_k :

$$\mathcal{L}_{\text{align}} = \|\mathbf{e}_k - \hat{\mathbf{e}}_k\|_2^2 \quad (2)$$

Second, to further transfer capabilities of teacher model, we employ the *Teacher-Forced Distillation Objective* ($\mathcal{L}_{\text{distill}}$). By utilizing the teacher model’s segmentation boundaries to synchronize the sequence lengths, we minimize the KL divergence between the student model’s and teacher model’s output distributions:

$$\mathcal{L}_{\text{distill}} = \sum_{k=1}^N D_{\text{KL}}(P_T(\cdot | \mathbf{t}_{<k}) \| P_S(\cdot | \mathbf{x}_{<\text{pos}(k)})) \quad (3)$$

Here, N denotes the total number of tokens in the sequence, $\mathbf{t}_{<k}$ represents the teacher model’s prefix tokens, and $\mathbf{x}_{<\text{pos}(k)}$ corresponds to the student model’s byte sequence up to the boundary index of the k -th token.

Third, to enable autonomous tokenization, we introduce the *Boundary Learning Objective* ($\mathcal{L}_{\text{boundary}}$), where the Routing Module is trained to predict token boundaries via binary classification on each byte:

$$\mathcal{L}_{\text{boundary}} = -\frac{1}{L} \sum_{i=1}^L [y_i \log(p_i) + (1 - y_i) \log(1 - p_i)] \quad (4)$$

where L is the total length of the byte sequence, $y_i \in \{0, 1\}$ is the ground-truth boundary label derived from the teacher tokenizer, and p_i is the predicted probability that byte i is a boundary.

Optimization Strategy. While a holistic objective $\mathcal{L}_{\text{total}} = \lambda_1 \mathcal{L}_{\text{align}} + \lambda_2 \mathcal{L}_{\text{distill}} + \lambda_3 \mathcal{L}_{\text{boundary}}$, as adopted in (Minixhofer et al., 2025a), is theoretically possible, it often leads to training instability due to the competition between boundary learning and semantic alignment and requires extensive hand-tuning of multiple hyperparameters.

In contrast, our framework adopts a *sequential curriculum* that eliminates these sensitivities:

1. **Encoder Alignment:** Optimize $\mathcal{L}_{\text{align}}$ to establish a foundational mapping from bytes to the teacher model’s space.
2. **Joint Distillation:** Train the Encoder and Core Transformer using $\mathcal{L}_{\text{distill}}$ to adapt the backbone to byte-derived representations.
3. **Boundary Learning:** Freeze the backbone and optimize $\mathcal{L}_{\text{boundary}}$ to finalize the Routing Module.

This curriculum ensures that each module is trained on top of a stable representation, making the framework highly robust and generalizable to diverse models without extensive hyperparameter searching.

Upon completion of this stage, the student model successfully learn to dynamically group raw bytes into chunks and generate in the token space.

4.2.2. STAGE 2: SFT FOR BYTE-TO-BYTE MODELING

The student model after Stage 1 still relies on a token LM head for generation, necessitating the subsequent stage for end-to-end byte generation. We replace the token LM head with *Dechunk* and *Decoder* modules and train the model using the Next Byte Prediction loss.

This process follows a two-step fine-tuning process. First, we perform *Head Adaptation*, training only the newly initialized Dechunk and Decoder modules to align with the distilled backbone representations. Subsequently, we proceed to *end-to-end fine-tuning*, where all parameters are unfrozen to optimize the entire model. This ensures that the model retains the linguistic richness acquired in Stage 1 while gaining the flexibility of pure byte-level modeling.

4.2.3. COMPARISON WITH BOLMO

Our framework diverges from the approach introduced in Bolmo (Minixhofer et al., 2025a) in two fundamental respects.

First, while Bolmo attempts to perform distillation in a single, end-to-end step, our framework decomposes this process into a sequential curriculum. We explicitly separate representation alignment and capability transfer from boundary learning: the model first aligns encoder representations and transfers capabilities from the teacher, after which the backbone is frozen to focus on learning dynamic

byte boundaries.

Second, the two methods adopt distinct distillation paradigms. Bolmo follows an end-to-end formulation in which the student model is trained to directly approximate the target byte-level distribution. In contrast, our approach introduces a deliberate intermediate stage, allowing the student model to first learn to dynamically group raw bytes into chunks while generating outputs in the token space. By retaining the teacher model’s token-level LM head during Stage 1, we explicitly align the student with the teacher’s token-level distribution before transitioning to fully byte-level generation in the final stage.

5. Experiments

Our experiments aim to verify the data efficiency of our two-stage curriculum and the plasticity of the model for post-training. Following the setup in Section 5.1, Section 5.2 demonstrates our framework’s superior performance against baselines such as BLT and H-Net, highlighting the critical role of the intermediate alignment stage. Finally, Section 5.3 validates the model’s extensibility through standard on-policy optimization.

5.1. Experimental Setup

Models and Architecture. To evaluate the universality of the proposed approach, experiments are conducted two open-weight model families: Llama-3.2 3B and Qwen-3 4B. These models function as token-trained LM teacher models. In the student models, the core transformer layers and language modeling head are initialized with the corresponding teacher model’s weights. Notice that all the models employ JBP decoding strategy mentioned in Sec 4.1.2. A detailed ablation study about these decoding strategy can be found in Sec 6.2. The detailed model configurations are provided in Appendix E.

Training Data. We utilize the FineWeb dataset (Penedo et al., 2024) for all training phases. Stage 1 is conducted on a 30B byte subset (approximately 7B tokens), which provides sufficient semantic coverage for knowledge transfer. For Stage 2, we further employ 95B bytes of data to refine the model’s autonomous generation capabilities. In total, our framework requires only 125B bytes of training data.

Evaluation Metrics. The performance is evaluated on a comprehensive suite of downstream benchmarks: HellaSwag (Zellers et al., 2019), PIQA (Bisk et al., 2019), ARC-Easy, ARC-Challenge (Clark et al., 2018), Winogrande (Sakaguchi et al., 2019), OpenBookQA (Mihaylov et al., 2018), and Massive Multitask Language Understanding (MMLU) (Hendrycks et al., 2021). We do all of the evaluations using *lm-evaluation-harness* (Gao et al., 2024) for reproducibility.

Table 1. Main Results: Comparison of Byte-Level Distillation Methods. We evaluate our two-stage recipe against leading baselines across various model families. **Avg Drop** measures the mean performance degradation relative to each method’s respective token-trained teacher model. Compared to existing baselines, our approach achieves higher performance retention using fewer training bytes.

Method	Role / Model	Bytes	Task Performance								Retention Avg Drop ↓	
			LMB	HellA	PIQA	ARC-E	ARC-C	WINO	Open	MMLU		
<i>Existing Leading Baselines</i>												
BLT Distill (Pagnoni et al., 2024)	Teacher (Llama 2 7B)	-	80.7	80.7	83.4	55.2	-	-	66.3	-	7.34	
	Student (Byte)	220B	-	76.1	77.4	66.6	45.8	-	-	63.7		
ALM (Minixhofer et al., 2025b)	Teacher (Llama 3.2 3B)	-	-	-	76.9	-	43.9	-	-	62.4	-	
	Student (Byte)	-	-	-	73.7	-	40.1	-	-	55.9	4.50	
H-Net Distill (Hwang et al., 2025)	Teacher (Llama 3.2 3B)	-	70.1	73.7	76.8	74.5	46.0	66.5	41.4	56.1	-	
	Student (Byte)	189B	63.4	70.2	76.1	72.1	43.3	66.5	41.4	51.9	9.85	
<i>Ours: Two-stage Distillation Pipeline</i>												
Ours (Llama 3.2 3B)	Teacher (Baseline)	-	70.1	73.7	76.8	74.6	46.0	66.5	41.4	56.0	-	
	Ours (Stage 1)	30B	69.5	72.9	76.1	73.6	43.9	67.2	41.1	51.6	1.15	
	Ours (Stage 2)	95B	69.3	71.2	73.7	69.5	41.9	65.9	39.4	51.8	2.80	
Ours (Qwen 3 4B)	Teacher (Baseline)	-	69.1	73.6	77.7	78.9	51.3	70.4	40.6	73.0	-	
	Ours (Stage 1)	30B	68.4	72.5	77.0	76.8	50.2	69.0	40.2	66.8	1.71	
	Ours (Stage 2)	95B	66.2	69.7	75.4	77.1	52.6	66.4	41.2	68.5	2.19	

Table 2. Impact of On-Policy Distillation in Stage 1. We compare the Llama-3.2 3B Instruct teacher model with its byte-level student model before and after on-policy distillation. On-Policy distillation improving performance across nearly all benchmarks and narrowing the gap with the teacher.

Model Phase	Role	LMB	HellA	PIQA	ARC-E	ARC-C	WINO	Open	MMLU
Baseline	Teacher	65.98	70.40	75.79	74.03	45.82	67.64	36.00	59.68
Stage I	Student	49.16	69.09	75.24	72.01	43.52	65.98	36.20	52.52
+ On-Policy	Student	55.95	69.44	76.06	72.52	45.05	66.93	36.00	54.64

Hyperparameters. Across all training stages, we utilize the AdamW optimizer with a cosine decay schedule and a weight decay of 0.1. The detailed hyperparameter configurations for each stage are provided in Appendix E.

5.2. Effectiveness of the Proposed Recipe

5.2.1. PERFORMANCE OF STAGE 1

Comparison with Leading Baselines. We evaluated our method against leading byte-level distillation baselines: BLT (Pagnoni et al., 2024), ALM (Minixhofer et al., 2025b), and H-Net (Hwang et al., 2025). Given the differences in base model capabilities, we report *Avg Drop* to isolate distillation efficiency from the varying strengths of teacher models, which is defined as the mean accuracy reduction of the student model relative to its specific teacher model across all tasks.

As shown in Table 1, our approach results in the lowest performance drop across all benchmarks. For Llama-3.2 3B and Qwen-3 4B, the degradation is limited to just 1.15 and 1.71 points, respectively, outperforming BLT (7.34 drop) and ALM (4.50 drop). Compared with H-Net, our student model achieves better retention with less data.

Analysis of Distillation Dynamics. We further plot the training dynamics in Stage 1. Figure 2 presents the evaluation accuracy during *Step 1 (Encoder Alignment)* and *Step 2 (Joint Distillation)*.

Step 1 (Rapid Alignment): The sharp increase to the left of the dash line demonstrates that aligning the encoder with the teacher model’s static embedding space effectively solve the boundary misalignment. This process is sufficient to recover the performance of surface-level tasks (e.g., PIQA) with less than 5 B bytes of data.

Step 2 (Reasoning Transfer): The shift to joint distillation is crucial for complex reasoning. While simple tasks reach a plateau, knowledge-intensive tasks such as MMLU and ARC-Challenge continue to show growth in performance. This confirms that while embedding alignment addresses modality, sequence-level distillation is vital for inheriting deep-semantic reasoning.

Data Efficiency. Table 1 shows the relationship between training data volume and accuracy. Our method achieves convergence with 30B bytes, a six-fold reduction from H-Net’s 189B bytes, while matching its downstream performance.

Table 3. Necessity of Stage 1 Embedding Alignment. We conduct an ablation using Llama-3.2 3B to evaluate the impact of embedding alignment before full distillation. Results show that omitting embedding alignment leads to a significant performance collapse across all benchmarks, confirming it as a critical foundation for our recipe.

Method	LMB	HellA	PIQA	ARC-E	ARC-C	WINO	Open
Baseline	69.9	73.8	76.7	74.6	46.8	67.4	41.4
Distill	70.7	73.6	76.2	74.3	44.9	69.4	41.2
Distill w/o emb	31.2	46.7	58.8	37.0	21.6	60.3	33.4

Table 4. Comparison of Decoding Strategies. We evaluate Joint Boundary Prediction (JBP) versus Multi-Byte Prediction (MBP) using the Qwen-based student model. Although MBP shows marginal gains on some common-sense tasks, JBP exhibits superior robustness in complex reasoning, as evidenced by the substantial performance lead in GSM8.

Decoding Strategy	LMB	HellA	PIQA	ARC-E	ARC-C	WINO	Open	MMLU	GSM8K
JBP	66.2	69.7	75.4	77.1	52.6	66.4	41.2	68.4	53.5
MBP	66.7	70.3	74.8	77.8	53.4	66.5	38.2	69.2	37.4

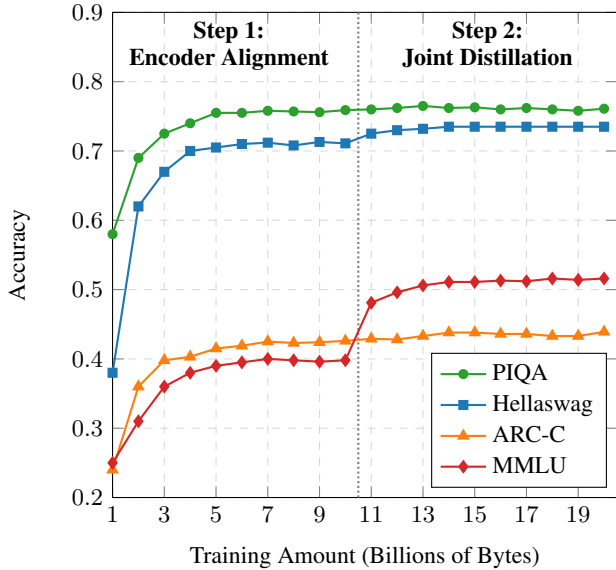


Figure 2. Training Dynamics across Stage 1. We track student performance in Stage 1. While simple tasks (e.g., PIQA) converge rapidly during Encoder Alignment (Step 1), knowledge-intensive tasks like MMLU exhibit a distinct phase transition, requiring the distribution matching of Joint Distillation (Step 2) to unlock performance gains.

5.2.2. PERFORMANCE OF STAGE 2

We summarize the comparison between our Stage 2 model and baseline results in Table 1. The results show superior capability retention of our recipe versus baseline methods. Our Llama-3.2 3B student model restricts *Avg Drop* to 2.80, outperforming H-Net Distill (9.85), BLT Distill (7.34), and ALM (4.50). This indicates effective mitigation of representation collapse in byte-level adaptation. Our method achieves this alignment with higher data efficiency than these baselines. The robustness extends across architectures, shown by low degradation (2.19) in our Qwen-3 4B stu-

dent model, confirming our two-stage distillation pipeline’s effectiveness over previous SFT approaches.

5.3. Applicability of Post-Training Techniques

To further validate the extensibility of our framework, we explore whether the Stage 1 model can be enhanced using standard post-training techniques. Specifically, we seek to determine whether the model can benefit from on-policy optimization to further address performance gaps or enhance reasoning capabilities.

Methodology. We adapt a hybrid approach that integrates *GOLD* (Patiño et al., 2025) with *On-Policy Distillation* (Lu & Lab, 2025). Although *GOLD* facilitates token-to-byte distillation, its theoretical effectiveness is linked to an overlap of the vocabularies of the models. This is where the architectural strength of the Stage 1 student model becomes apparent. The learned *Routing Module* achieves exceptionally high boundary detection accuracy compared to the teacher model, ensuring that the student model’s dynamic segmentation trajectory closely aligns with that of the teacher model. This precise alignment meets the requirements of the *GOLD* algorithm, allowing for effective on-policy learning despite architectural differences.

In our implementation, we employ a subset of 77k prompts from the *Tulu V3 Mix* dataset (Lambert et al., 2024). We unfrozen the entire Stage 1 model and optimized it using AdamW with a learning rate of 2×10^{-5} and a cosine decay schedule. To maintain the stability of the *Routing Module* during these updates, we integrated the Binary Cross-Entropy (BCE) loss from Stage 1 as an auxiliary objective. We utilized *Llama-3.2 3B Instruct* model as the teacher model to assess the transfer of instruction following and the reasoning capabilities of the model.

Results. As illustrated in Table 2, the implementation of *GOLD* and On-Policy distillation consistently boosts per-

Table 5. Impact of Encoder Architecture. We compare the performance of Mamba2 against a standard Transformer encoder. Results indicate that the Transformer’s attention mechanism struggles to align fine-grained byte sequences with high-level semantic embeddings, leading to a significant performance collapse, particularly on knowledge-intensive benchmarks like MMLU.

Encoder	LMb	HellA	PIQA	ARC-E	ARC-C	WINO	Open	MMLU
Mamba2	67.8	73.5	78.2	77.1	49.7	69.5	40.0	70.2
Transformer	45.7	68.3	73.3	69.4	44.5	66.2	37.4	31.3

formance across various benchmarks. This enhancement is particularly pronounced in reasoning tasks, which effectively aids in knowledge recovery, reducing the performance gap on demanding tasks such as MMLU by increasing the score from 52.52 to 54.64. These findings indicate that the Stage 1 architecture offers a solid foundation that is fully compatible with advanced optimization techniques.

6. Ablation Study

6.1. Necessity of Embedding Alignment

In Stage 1, our framework employs a sequential optimization strategy comprising three steps: embedding alignment, distillation, and boundary learning. To assess the necessity of the initial *embedding alignment* step, we conduct an ablation study using Llama-3.2 3B as the teacher model.

Experimental Setup. We compare two configurations under a fixed compute budget of 20B bytes: (1) **Distill (Sequential)**: The model underwent 10B bytes of embedding alignment, followed by 10B bytes of distillation. (2) **Distill w/o emb**: The model skips the alignment step and undergoes 20B bytes of direct distillation. For both settings, the learning rates are consistently set to 1×10^{-3} for the encoder and 2×10^{-5} for the main transformer. The evaluation results for multiple benchmarks are presented in Table 3.

Analysis. The result reveals that omitting the embedding alignment results in catastrophic failure in knowledge transfer. The *Distill w/o emb* variant exhibits a drastic performance decline, with the LMB score decreasing from 70.7 to 31.2.

This collapse highlights a key challenge in token-to-byte distillation: byte-level student model and token-trained teacher model initially occupy different latent spaces. Without *embedding alignment* to bridge this gap, the student model’s transformer cannot interpret latent states during distillation. Anchoring the student model’s embedding space to the teacher model’s enables effective transfer of capabilities.

6.2. Ablation Study on Decoding Strategy

We investigate the impact of the decoding strategy used in Stage 2. Specifically, we compare the *JBP* and *MBP* strategies, as detailed in Section 4.1.2.

The results are summarized in Table 4. While MBP achieves marginal gains on several benchmarks (e.g., +0.8% on MMLU), it suffers from a performance degradation on GSM8K (Cobbe et al., 2021) (53.5% vs. 37.4%). This result directly indicates that the MBP decoding mechanism is ineffective for long-horizon autoregressive generation. The reliance on an auxiliary head and similarity-based routing struggles to maintain the coherence required for complex reasoning chains.

Consequently, we adopt JBP as the default strategy to ensure the model’s capabilities.

6.3. Impact of Encoder Architecture

A pivotal design choice in this framework is the selection of *Mamba2* as the encoder. To substantiate this decision, an ablation study is conducted in which the Mamba2 block is substituted with a standard transformer of equivalent parameter size. Both encoder variants are trained using the same *Step 1 (Embedding Alignment)* protocol on Qwen-3 4B.

Performance Collapse of Attention. Table 5 shows significant differences in alignment quality. The Mamba2 encoder achieves high fidelity (70.2 MMLU), while the transformer variant shows performance decline in knowledge-intensive tasks (31.3 MMLU). This disparity stems from byte sequences characteristics. Raw byte streams are longer than token sequences, reducing attention mechanism’s ability to capture semantic structures, while the State Space Model (SSM) backbone of Mamba2 can effectively compresses these signals into meaningful latent states.

7. Conclusion

In this paper, we propose a practical two-stage distillation framework that converts pretrained token-based LLMs into byte-level models while preserving most of their capabilities. Our method is effective across multiple model families, including Llama, Qwen, and OLMo, and achieves competitive performance using only 125B training bytes, substantially lowering the cost of building scalable BLMs.

8. Impact Statement

This paper presents work whose goal is to advance the field of machine learning. There are many potential societal

consequences of our work, none of which we feel must be specifically highlighted here.

References

Bisk, Y., Zellers, R., Bras, R. L., Gao, J., and Choi, Y. Piqa: Reasoning about physical commonsense in natural language, 2019. URL <https://arxiv.org/abs/1911.11641>.

Clark, P., Cowhey, I., Etzioni, O., Khot, T., Sabharwal, A., Schoenick, C., and Tafjord, O. Think you have solved question answering? try arc, the ai2 reasoning challenge, 2018. URL <https://arxiv.org/abs/1803.05457>.

Cobbe, K., Kosaraju, V., Bavarian, M., Chen, M., Jun, H., Kaiser, L., Plappert, M., Tworek, J., Hilton, J., Nakano, R., et al. Training verifiers to solve math word problems. *arXiv preprint arXiv:2110.14168*, 2021.

Dao, T. and Gu, A. Transformers are ssms: Generalized models and efficient algorithms through structured state space duality, 2024. URL <https://arxiv.org/abs/2405.21060>.

Egli, E., Manica, M., and Born, J. Multiscale byte language models—a hierarchical architecture for causal million-length sequence modeling. *arXiv preprint arXiv:2502.14553*, 2025.

Gao, L., Tow, J., Abbasi, B., Biderman, S., Black, S., DiPofi, A., Foster, C., Golding, L., Hsu, J., Le Noac'h, A., Li, H., McDonell, K., Muennighoff, N., Ociepa, C., Phang, J., Reynolds, L., Schoelkopf, H., Skowron, A., Sutawika, L., Tang, E., Thite, A., Wang, B., Wang, K., and Zou, A. The language model evaluation harness, 07 2024. URL <https://zenodo.org/records/12608602>.

Grattafiori, A., Dubey, A., Jauhri, A., et al. The llama 3 herd of models, 2024. URL <https://arxiv.org/abs/2407.21783>.

Hendrycks, D., Burns, C., Basart, S., Zou, A., Mazeika, M., Song, D., and Steinhardt, J. Measuring massive multitask language understanding, 2021. URL <https://arxiv.org/abs/2009.03300>.

Hinton, G., Vinyals, O., and Dean, J. Distilling the knowledge in a neural network, 2015. URL <https://arxiv.org/abs/1503.02531>.

Ho, N., Bae, S., Kim, T., Jo, H., Kim, Y., Schuster, T., Fisch, A., Thorne, J., and Yun, S.-Y. Block transformer: Global-to-local language modeling for fast inference. *Advances in Neural Information Processing Systems*, 37:48740–48783, 2024.

Hwang, S., Wang, B., and Gu, A. Dynamic chunking for end-to-end hierarchical sequence modeling, 2025. URL <https://arxiv.org/abs/2507.07955>.

Kasai, J., Peng, H., Zhang, Y., Yogatama, D., Ilharco, G., Pappas, N., Mao, Y., Chen, W., and Smith, N. A. Fine-tuning pretrained transformers into rnns. *arXiv preprint arXiv:2103.13076*, 2021.

Katharopoulos, A., Vyas, A., Pappas, N., and Fleuret, F. Transformers are rnns: Fast autoregressive transformers with linear attention. In *International conference on machine learning*, pp. 5156–5165. PMLR, 2020.

Lambert, N., Morrison, J., Pyatkin, V., Huang, S., Ivison, H., Brahman, F., Miranda, L. J. V., Liu, A., Dziri, N., Lyu, S., Gu, Y., Malik, S., Graf, V., Hwang, J. D., Yang, J., Bras, R. L., Tafjord, O., Wilhelm, C., Soldaini, L., Smith, N. A., Wang, Y., Dasigi, P., and Hajishirzi, H. Tülu 3: Pushing frontiers in open language model post-training. 2024.

Lu, K. and Lab, T. M. On-policy distillation. *Thinking Machines Lab: Connectionism*, 2025. doi: 10.64434/tml-20251026. <https://thinkingmachines.ai/blog/on-policy-distillation>.

Mihaylov, T., Clark, P., Khot, T., and Sabharwal, A. Can a suit of armor conduct electricity? a new dataset for open book question answering, 2018. URL <https://arxiv.org/abs/1809.02789>.

Minixhofer, B., Murray, T., Limisiewicz, T., Korhonen, A., Zettlemoyer, L., Smith, N. A., Ponti, E. M., Soldaini, L., and Hofmann, V. Bolmo: Byteifying the next generation of language models, 2025a. URL <https://arxiv.org/abs/2512.15586>.

Minixhofer, B., Vulić, I., and Ponti, E. M. Universal cross-tokenizer distillation via approximate likelihood matching, 2025b. URL <https://arxiv.org/abs/2503.20083>.

Nawrot, P., Tworkowski, S., Tyrolski, M., Kaiser, Ł., Wu, Y., Szegedy, C., and Michalewski, H. Hierarchical transformers are more efficient language models. In *Findings of the Association for Computational Linguistics: NAACL 2022*, pp. 1559–1571, 2022.

Nawrot, P., Chorowski, J., Lancucki, A., and Ponti, E. M. Efficient transformers with dynamic token pooling. In *Proceedings of the 61st Annual Meeting of the Association for Computational Linguistics (Volume 1: Long Papers)*, pp. 6403–6417. Association for Computational Linguistics, 2023a. doi: 10.18653/v1/2023.acl-long.353. URL <http://dx.doi.org/10.18653/v1/2023.acl-long.353>.

Nawrot, P., Chorowski, J., Lancucki, A., and Ponti, E. M. Efficient transformers with dynamic token pooling. In *Proceedings of the 61st Annual Meeting of the Association for Computational Linguistics (Volume 1: Long Papers)*, pp. 6403–6417, 2023b.

OLMo, T., Walsh, P., Soldaini, L., Groeneveld, D., Lo, K., Arora, S., Bhagia, A., Gu, Y., Huang, S., Jordan, M., et al. 2 olmo 2 furious. *arXiv preprint arXiv:2501.00656*, 2024.

Olmo, T., Ettinger, A., Bertsch, A., Kuehl, B., Graham, D., Heineman, D., Groeneveld, D., Brahman, F., Timbers, F., Ivison, H., et al. Olmo 3. *arXiv preprint arXiv:2512.13961*, 2025.

Pagnoni, A., Pasunuru, R., Rodriguez, P., Nguyen, J., Muller, B., Li, M., Zhou, C., Yu, L., Weston, J., Zettlemoyer, L., Ghosh, G., Lewis, M., Holtzman, A., and Iyer, S. Byte latent transformer: Patches scale better than tokens, 2024. URL <https://arxiv.org/abs/2412.09871>.

Patiño, C. M., Rasul, K., Gallouédec, Q., Burtenshaw, B., Paniego, S., Srivastav, V., Frere, T., Beeching, E., Tunstall, L., von Werra, L., and Wolf, T. Unlocking on-policy distillation for any model family, 2025.

Penedo, G., Kydlíček, H., allal, L. B., Lozhkov, A., Mitchell, M., Raffel, C., Werra, L. V., and Wolf, T. The fineweb datasets: Decanting the web for the finest text data at scale. In *The Thirty-eight Conference on Neural Information Processing Systems Datasets and Benchmarks Track*, 2024. URL <https://openreview.net/forum?id=n6SCkn2QaG>.

Sakaguchi, K., Bras, R. L., Bhagavatula, C., and Choi, Y. Winogrande: An adversarial winograd schema challenge at scale, 2019. URL <https://arxiv.org/abs/1907.10641>.

Slagle, K. Spacebyte: Towards deleting tokenization from large language modeling. *Advances in Neural Information Processing Systems*, 37:124925–124950, 2024.

Vaswani, A., Shazeer, N., Parmar, N., Uszkoreit, J., Jones, L., Gomez, A. N., Kaiser, Ł., and Polosukhin, I. Attention is all you need. *Advances in neural information processing systems*, 30, 2017.

Wang, J., Gangavarapu, T., Yan, J. N., and Rush, A. M. Mambabyte: Token-free selective state space model, 2024a. URL <https://arxiv.org/abs/2401.13660>.

Wang, J., Paliotta, D., May, A., Rush, A., and Dao, T. The mamba in the llama: Distilling and accelerating hybrid models. *Advances in Neural Information Processing Systems*, 37:62432–62457, 2024b.

Yang, A., Li, A., Yang, B., Zhang, B., Hui, B., Zheng, B., Yu, B., Gao, C., Huang, C., Lv, C., Zheng, C., Liu, D., Zhou, F., Huang, F., Hu, F., Ge, H., Wei, H., Lin, H., Tang, J., Yang, J., Tu, J., Zhang, J., Yang, J., Yang, J., Zhou, J., Zhou, J., Lin, J., Dang, K., Bao, K., Yang, K., Yu, L., Deng, L., Li, M., Xue, M., Li, M., Zhang, P., Wang, P., Zhu, Q., Men, R., Gao, R., Liu, S., Luo, S., Li, T., Tang, T., Yin, W., Ren, X., Wang, X., Zhang, X., Ren, X., Fan, Y., Su, Y., Zhang, Y., Zhang, Y., Wan, Y., Liu, Y., Wang, Z., Cui, Z., Zhang, Z., Zhou, Z., and Qiu, Z. Qwen3 technical report, 2025. URL <https://arxiv.org/abs/2505.09388>.

Yu, L., Simig, D., Flaherty, C., Aghajanyan, A., Zettlemoyer, L., and Lewis, M. Megabyte: Predicting million-byte sequences with multiscale transformers. *Advances in Neural Information Processing Systems*, 36:78808–78823, 2023.

Zellers, R., Holtzman, A., Bisk, Y., Farhadi, A., and Choi, Y. Hellaswag: Can a machine really finish your sentence?, 2019. URL <https://arxiv.org/abs/1905.07830>.

A. In-depth Analysis of Byte-level Robustness and Boundary Learning

In this section, we provide a comprehensive evaluation of the robustness of the distilled H-Net and investigate the behavioral patterns of its boundary predictor.

A.1. Intrinsic Byte-level Resilience

Traditional LLMs depend on subword tokenization, which is inherently vulnerable to surface-level disturbances; even slight character-level noise can significantly change token IDs, resulting in semantic collapse. In contrast, byte-level modeling processes raw sequences, theoretically providing greater granularity and robustness. While our distillation framework has been demonstrated to effectively maintain the teacher model’s semantic performance on standard benchmarks (as discussed in Section 5), it is crucial to assess whether the distilled H-Net genuinely inherits the distinctive resilience characteristics of byte-level architectures.

Following the methodology proposed in BLT (Pagnoni et al., 2024), we assess our models using the HellaSwag benchmark, focusing on five types of character-level perturbations: *AntSpeak*, *Drop*, *Random Case*, *Repeat*, and *Uppercase*. Furthermore, we add a *Robustness Score* proposed by H-Net (Hwang et al., 2025) as a metric, which is calculated as follows:

$$\text{robustness score} = 100 \cdot \left(\frac{\text{perturbed accuracy} - 0.25}{\max(\text{unperturbed accuracy} - 0.25, 0)} \right) \quad (5)$$

As shown in Table 6, our distilled Stage 1 models demonstrate a significant level of intrinsic resilience. For Llama-3.2 3B, while the teacher model baseline performs well on clean text, the Stage1 model achieves higher accuracy on several noise types, such as *AntSpeak* (48.78 vs. 46.62) and *Drop* (52.30 vs. 52.03). This indicates that the distillation process does more than merely replicate the teacher model’s probability distribution; it enables the H-Net to utilize its byte-to-byte architecture to bypass the fragility of the subword boundaries. Interestingly, the Stage2 models exhibit a decrease in robustness compared to Stage1, particularly in benchmarks such as *AntSpeak*. This suggests that while further fine-tuning maintains the overall performance, it may introduce a degree of boundary fragility, making the model more sensitive to certain structural perturbations.

Table 6. Robustness Evaluation on HellaSwag. We reported zero-shot accuracy across the five perturbation types. **Robustness Score** is the harmonic mean of clean and noisy performance (higher is better). **Bold** indicates the best performance within each model family.

Metric / Model	Qwen-3 4B			Llama-3.2 3B		
	Baseline	Stage1	Stage2	Baseline	Stage1	Stage2
HellaSwag Original	73.64	72.47	69.70	73.76	72.90	71.20
HellaSwag Noise Avg	58.22	56.25	48.86	54.10	53.29	51.40
Robustness Score	68.29	65.83	53.38	59.68	59.06	57.14
<i>Breakdown by Perturbation Type</i>						
AntSpeak	59.86	57.02	45.48	46.62	48.78	38.05
Drop	52.94	55.03	46.42	52.03	52.30	48.71
Random Case	59.27	54.55	48.89	53.76	51.77	49.61
Repeat	50.27	50.36	42.44	49.05	48.74	43.17
Uppercase	68.80	64.26	61.08	69.12	64.83	62.93

A.2. Boundary Analysis and Optimization Strategies

Despite the intrinsic resilience observed in the intermediate distillation stage, the integration of an explicit boundary predictor leads to a noticeable decline in the overall robustness score compared to the teacher model baseline. To investigate this performance gap, we conducted a qualitative analysis of the segmentation behavior of the model under various input conditions.

Visualization of Boundary Bias. By visualizing the predicted boundaries (see Figure 3), we discovered that the model’s segmentation is heavily overfitted to a specific surface pattern: it consistently predicts boundaries at the character immediately preceding a whitespace. This *Space Bias* suggests that the boundary predictor prioritizes shallow lexical cues over deep semantic segmentation. While this heuristic works for clean text, it becomes liable in the presence of perturbations. For

instance, in *AntSpeak*, the proliferation of spaces forces the model to segment at every character, whereas in *Drop*, the removal of spaces leaves the model unable to identify logical segments, thereby disrupting the downstream transformer’s processing.

Proposed Mitigation Strategies. To alleviate this bias and force the model to learn more robust semantic-oriented segmentation, we propose two strategies.

1. **Trim Data:** We fine-tune the model on a modified dataset where all whitespaces are removed, forcing the model to rely on character sequences alone to determine boundaries.
2. **Whitespace Penalty:** We introduce a penalty term in the boundary loss function to discourage the model from triggering boundaries at whitespace positions, thereby encouraging the exploration of alternative semantic anchor points.

Results Analysis. The results in Table 7 reveal a clear trade-off between clean-text accuracy and noise invariance. The **Trim Data** strategy successfully recovers most of the robustness lost during standard boundary learning, maintaining a stable robustness score of 59.39. Remarkably, the **Whitespace Penalty** achieves the lowest sensitivity to noise ($\Delta = 14.45$), effectively creating a “noise-invariant” boundary predictor. However, this stability comes at the cost of a significant drop in *Original* performance (58.50), indicating that while penalizing space boundaries enhances resilience, it may also prevent the model from identifying the standard linguistic boundaries necessary for clean-text reasoning. These findings highlight the challenge of balancing the structural adherence and robustness in byte-level LLMs.

Table 7. Evaluation of boundary optimization strategies on Llama-3.2 3B. We compare our proposed **Trim Data** and **Whitespace Penalty** against the teacher model baseline and the standard boundary learning stage. **Delta** (Δ) indicates the performance gap between original and noisy benchmarks.

Metric / Model	Llama (Teacher Model)	Llama Distill Stage 1	Llama Trim Data	Llama Space Penalty
HellaSwag Original	73.76	72.90	72.57	58.50
HellaSwag Noise Avg	54.10	53.29	53.25	44.05
Robustness Score	59.68	59.06	59.39	53.66
Delta (Δ)	19.66	19.61	19.32	14.45
AntSpeak	46.62	48.78	48.76	39.26
Drop	52.94	52.30	54.03	44.19
Random Case	53.76	51.77	51.59	43.39
Repeat	49.05	48.74	48.19	41.29
Uppercase	69.12	64.83	63.70	52.10

A.3. Finetuning on Perturbed Benchmarks: A Limit Study

To further investigate the performance limits and adaptation capabilities of different architectures, we conducted a supervised fine-tuning (SFT) experiment. We compare the subword-level Llama (Token) against our distilled byte-level H-Net (Distill) by fine-tuning both on the perturbed HellaSwag training set.

Experimental Setup. Both models are fine-tuned for 10 epochs with a learning rate of 2×10^{-5} and a weight decay of 0.1. This setup aims to assess whether the subword model can “learn” to be robust through data augmentation, and how the byte-level model compares in this intensive adaptation scenario. The results are presented in Table 8.

Analysis. The experimental results highlight the fundamental differences in the adaptability of the two architectures. Notably, the byte-level *Llama distill* model exhibited a significantly higher adaptation ceiling than its subword counterpart. After fine-tuning, it achieved the highest overall Robustness Score (69.93) and consistently surpassed the teacher model across the averaged noise metrics. Critical divergence is evident in the *AntSpeak* task, which serves as a litmus test for tokenizer rigidity. While the subword model’s performance remains stagnant at 46.59, despite ten epochs of specific training—underscoring a “hard bottleneck” imposed by fixed vocabulary constraints—our byte-level model successfully adapts to the character-spaced inputs, increasing from 49.05 to 56.07. Furthermore, the byte-level architecture demonstrates superior stability to catastrophic forgetting. Whereas the subword model experiences a decline in clean-text performance (dropping from 73.76 to 71.90) as it struggles to accommodate noisy patterns, the distilled model maintains its original

Table 8. Comparison of subword-level (*Llama token*) and byte-level (*Llama distill*) models after fine-tuning on perturbed HellaSwag. *Origin* denotes zero-shot performance without noise-specific tuning, while *Finetune* denotes performance after 10 epochs of training on noisy data.

Metric	Origin			Finetuned		
	Token	Distill	Dechunk	Token	Distill	Dechunk
HellaSwag Original	73.76	73.50	71.38	71.90	73.58	70.90
HellaSwag Noise Avg	54.10	55.30	47.47	57.23	58.97	56.67
Robustness Score	59.68	62.40	48.46	68.72	69.93	69.00
Delta (Δ)	19.66	18.26	23.91	14.67	14.61	14.23
AntSpeak	46.62	49.05	32.32	46.59	56.07	55.64
Drop	52.03	56.21	49.20	59.32	58.30	51.74
Random Case	53.76	53.41	48.06	57.61	56.40	60.70
Repeat	49.05	50.71	44.35	58.55	56.38	50.57
Uppercase	69.12	66.79	63.44	64.10	67.68	64.71

capabilities (73.58), suggesting that its granular representation space allows the integration of noisy features without overwriting the structural knowledge required for standard reasoning.

B. Decoupled vs. Integrated Routing Module

In the proposed H-Net design, the routing module is seamlessly integrated within the encoder to utilize hidden representations to predict the token boundaries. However, an intriguing alternative is to consider whether the routing logic can be separated from the main semantic encoder to operate as an independent component. To explore this, we developed a decoupled routing module comprising a 4-layer Mamba2 block with a hidden dimension of 512, followed by a linear layer and sigmoid activation head for direct binary boundary classification from raw byte sequences. This standalone router was trained using the same dataset and hyperparameters as in our Stage 1 distillation process.

The experimental results, as outlined in Table 9, highlight a notable performance gap between the integrated and decoupled approaches. Most strikingly, the *Lambda* task score for the split routing module falls to 39.05, marking a significant decline from the 58.65 achieved by our integrated Stage 1 model. This downward trend is evident across all downstream benchmarks, including HellaSwag, PIQA, and ARC, where the decoupled model lagged consistently.

The observed decline in performance suggests that token boundaries in natural language are not merely local morphological features that can be captured using a shallow, independent module. Rather, the detection of these boundaries is heavily dependent on high-level semantic and syntactic contexts that only a fully developed encoder can provide. When the routing module is compelled to operate in isolation, the system loses the benefit of "feature sharing" between representation learning and structural segmentation. Consequently, even minor inaccuracies in the standalone router's predictions can result in significant chunking errors, leading to the subsequent encoder receiving fragmented byte segments that are no longer aligned with the teacher model's original semantic space. These findings support our architectural decision to integrate the routing mechanism within the hierarchical encoder, because the synergy between semantic understanding and boundary discovery is essential for maintaining the integrity of knowledge transfer in byte-level modeling.

Table 9. Comparison of performance between the integrated routing module (Stage 1) and a decoupled (Split) routing module. The baseline is the teacher model, Llama 3.2 3B.

Method	LMB	HellA	PIQA	ARC-E	ARC-C	WINO	Open
Baseline (Teacher)	69.9	73.8	76.7	74.6	46.8	67.4	41.4
Integrated	58.7	72.9	76.1	73.6	43.9	68.0	40.2
Split Routing	39.1	68.2	75.3	70.4	39.9	62.8	36.4

C. Teacher Model Scale during Stage 1 Alignment

In the first stage of our curriculum, we focus on aligning byte-level representations with the latent space of the teacher model. To determine whether the scale of the teacher model plays a decisive role in this process, we evaluated three distinct student-teacher configurations: Llama 3.2 1B distilled from a 3B teacher model and Qwen3 0.6B and 4B distilled from their 4B and 8B versions, respectively. The objective was to observe whether the increased capacity of a larger teacher model translates into more robust representational guidance for byte-level student models.

The comparative results summarized in Table 10 reveal that employing a significantly larger teacher model does not offer a distinct advantage; rather, it frequently results in a consistent decline in performance across all evaluation metrics. Within the Llama and Qwen families, the standard distillation setup, in which the teacher model is of a similar scale, consistently produces better outcomes than larger teacher model variants.

Several factors may explain why larger teacher models do not necessarily enhance distillation outcomes in this context. Notably, contemporary small-scale models, such as Llama 3.2 and Qwen3, often result from the extensive distillation of much larger "frontier" models. This suggests that their latent spaces are highly optimized and information-dense. When a student model is distilled from a slightly larger model within the same family, the potential for "knowledge gain" is limited, while the risk of introducing subtle representational noise or latent misalignments increases. Such discrepancies can complicate student models' learning of byte-to-token mapping, ultimately affecting the overall modeling quality. These findings support our architectural decision to prioritize scale consistency between student models and teacher models as it ensures a more seamless transfer of semantic knowledge during the critical alignment phase.

Table 10. Comparison of performance across different student-teacher scale configurations. "Baseline" refers to the original subword model and "Distill (Teacher X)" indicates distillation from a larger teacher model.

Student Model Method		LMB	HellA	PIQA	ARC-E	ARC-C	WINO	OpenMMLU	GSM8K
Llama 3.2 1B	Baseline	62.2	63.8	74.2	65.3	36.0	60.0	36.6	31.0
	Stage1	60.1	63.1	75.2	66.4	35.8	60.7	35.6	30.5
	Stage1 (Teacher 3B)	56.9	61.9	75.1	66.8	34.9	59.8	35.2	30.1
Qwen3 4B	Baseline	69.1	73.6	77.8	78.9	51.3	70.4	40.6	73.0
	Stage1	69.7	73.6	77.8	78.1	50.9	70.0	40.4	71.9
	Stage1 (Teacher 8B)	67.1	72.0	77.9	80.0	54.8	68.8	40.4	77.4
Qwen3 0.6B	Baseline	53.7	53.8	69.6	65.6	38.6	59.0	34.6	52.5
	Stage1	53.5	52.8	70.1	67.3	38.1	58.3	35.6	51.1
	Stage1 (Teacher 4B)	50.1	51.3	69.6	69.0	37.7	58.4	33.6	50.6

D. Detailed Comparison with Bolmo and Other Baselines

In this section, we extend our evaluation to include Bolmo 1B alongside other baselines such as BLT 1B and Hnet XL. As shown in Table 11, Bolmo 1B demonstrates strong capabilities, achieving an average accuracy of 60.3% across the 7 downstream tasks. When comparing our fully byte-level model (Ours Stage 2) against this baseline, we observe a performance gap, with our model attaining an average score of 58.1%. Specifically, Bolmo 1B outperforms our Stage 2 model on reasoning-heavy benchmarks such as ARC (59.0% vs. 55.5%) and HellaSwag (67.0% vs. 62.5%). However, our distilled model remains competitive on knowledge-intensive tasks, slightly surpassing Bolmo on MMLU (37.6% vs. 37.2%). We also note that BLT 1B remains the strongest baseline in this evaluation suite with an average score of 62.8%. These results provide a comprehensive view of the current landscape, highlighting that while our distillation framework effectively constructs a functional byte-level model, there remains room for improvement to match the performance of models trained with different objectives or larger computational budgets.

E. Training Hyperparameters

Full architecture hyperparameters are shown in Table 12, and full training in Table 13.

Table 11. Performance comparison on downstream tasks. We compare our proposed models (Stage 1 & Stage 2) with Bolmo 1B, Hnet XL variants, BLT 1B, and the sub-word reference. The best results among byte-level models are **bolded**.

Task	Ours (Stage 1)	Ours (Stage 2)	Bolmo	Hnet (1-stage)	Hnet (2-stage)	BLT	OLMo 2
Avg	60.3	58.1	60.3	57.6	59.2	62.8	61.9
ARC	60.0	55.5	59.0	61.8	62.3	59.9	61.4
MMLU	37.6	37.6	37.2	37.5	38.7	40.6	40.4
CSQA	65.8	62.6	64.2	61.4	62.4	69.2	66.0
HellaSwag	65.4	62.5	67.0	60.2	63.6	71.0	68.9
WinoGrande	63.9	63.5	65.7	58.9	60.9	67.0	65.2
SocialIQA	53.8	52.9	54.7	50.1	52.9	54.6	55.1
PiQA	75.7	72.3	74.9	73.6	74.0	77.3	76.4



Figure 3. Visualization of Learned Token Boundaries.

Table 12. Student model architecture details.

	H-net 4B	H-Net 3B	H-Net 1B
Global Model			
	Llama 3.2 3B	Qwen 3 4B	OLMo 2 1B
Encoder			
Dimension	1536	1536	1536
Layer Type	Mamba2 + FFN	Mamba2 + FFN	Mamba2 + FFN
Num. Layers	4	4	4
Mamba2			
chunk_size	256	256	256
d_conv	4	4	4
d_state	128	128	128
expand	2	2	2
FFN			
Expansion Dim.	8192	8192	8192
Nonlinearity	SwiGLU	SwiGLU	SwiGLU
Layer norm	RMSNorm	RMSNorm	RMSNorm
Local Decoder			
Dimension	1536	1536	1536
Layer Type	Mamba2 + FFN	Mamba2 + FFN	Mamba2 + FFN
Num. Layers	4	4	4
Mamba2			
chunk_size	256	256	256
d_conv	4	4	4
d_state	128	128	128
expand	2	2	2
FFN			
Expansion Dim.	8192	8192	8192
Nonlinearity	SwiGLU	SwiGLU	SwiGLU
Layer norm	RMSNorm	RMSNorm	RMSNorm

Table 13. Training details.

	Llama 3.2 3B	Qwen 3 4B	OLMo 2 1B
Stage 1			
Total Training Bytes	30B	30B	30B
Batch Size	256	256	256
Seq. Length. (Bytes)	8192	8192	8192
LR Schedule	Warmup + Cos Decay	Warmup + Cos Decay	Warmup + Cos Decay
Step 1			
Peak LR	1e-3	1e-3	1e-3
Warmup Ratio	0.2	0.2	0.2
Step 2			
Peak LR	2e-5	2e-5	2e-5
Warmup Ratio	0.01	0.01	0.01
Step 3			
Peak LR	1e-3	1e-3	1e-3
Warmup Ratio	0.1	0.1	0.1
Weight Decay	0.1	0.1	0.1
Optimizer	AdamW	AdamW	AdamW
β_1, β_2	0.9, 0.95	0.9, 0.95	0.9, 0.95
Max. Grad. Norm	1.0	1.0	1.0
Stage 2			
Total Training Bytes	95B	95B	95B
Batch Size	256	256	256
Seq. Length. (Bytes)	8192	8192	8192
LR Schedule	Warmup + Cos Decay	Warmup + Cos Decay	Warmup + Cos Decay
Step 1			
Peak LR (Decoder)	1e-3	1e-3	1e-3
Warmup Ratio	0.1	0.1	0.1
Step 2			
Peak LR (Encoder + Decoder)	4e-5	4e-5	4e-5
Peak LR (Main Transformer)	2e-5	2e-5	2e-5
Warmup Ratio	0.01	0.01	0.01
Weight Decay	0.1	0.1	0.1
Optimizer	AdamW	AdamW	AdamW
β_1, β_2	0.9, 0.95	0.9, 0.95	0.9, 0.95
Max. Grad. Norm	1.0	1.0	1.0